

**ORIGINAL ARTICLE**

**STRUCTURAL, ELECTRICAL AND PHOTOELECTROCHEMICAL PROPERTIES OF  
PULSE PLATED  $\text{CuIn}_{0.7}\text{Al}_{0.3}\text{Se}_2$  THIN FILMS**

<sup>1</sup>K.Ramesh, <sup>\*2</sup>M.Thirumoorthy and <sup>3</sup>K.R.Murali

<sup>1</sup>Department of Physics, Government Arts College, C-Mutlur, 608102,Chidambaram

<sup>2</sup>Department of Physics, Bannari Amman Institute of Technology, Sathy 638401, India

<sup>3</sup>Department of Theoretical Physics, University of Madras, Chennai, India

*Article History: Received 4<sup>th</sup> May,2017, Accepted 31<sup>st</sup> May,2017, Published 1<sup>st</sup> June,2017*

**ABSTRACT**

$\text{CuIn}_{0.7}\text{Al}_{0.3}\text{Se}_2$  films were deposited by pulse plated technique on indium tin oxide coated glass substrates at different duty cycles from 6 to 50% for the first time. The CIAS films were single phase by chalcopyrite structure. The crystallite size of the films increased from 17 nm – 42 nm with the decreases of duty cycle. Optical absorption measurements showed a band gap in the range of 1.17 eV to 1.51 eV with increase of duty cycle. Transmission spectra exhibited interference fringes. Using the envelope method, refractive index (n) value was calculated. The refractive index of the film increased with increase of duty cycle. Photoelectrochemical cells were made-up by using the films deposited at different duty cycle. Polysulphide redox electrolyte was used for the studies. To induce photoactivity of the films by post heat treated in argon atmosphere at different temperatures in the range of 450°C - 550°C. The films post heat treated at 525°C exhibited maximum photooutput. The films were photoetched in dilute 1:100  $\text{HNO}_3$ . The photooutput was  $V_{oc}$  of 0.75V,  $J_{sc}$  of 21.00  $\text{mA cm}^{-2}$ , ff of 0.62 and efficiency of 12.21 % at 60  $\text{mW cm}^{-2}$  illumination from tungsten halogen lamp after photoetching.

**Keywords:** Thin films, electronic material, semiconductor, I-III-VI<sub>2</sub>

**1.INTRODUCTION**

The development of renewable energy sources is one of the most pressing challenges the world currently faces. Proven coal reserves are estimated to last about another 120 years at current production rates while proven oil and gas reserves work out to near 45 to 60 years respectively. Of course, if these numbers are correct, as each reserve runs out, consumption of the remaining types of fuel will increase, shortening the time remaining until depletion. These numbers are also based on current production rates, and it would be unrealistic for production to remain at these levels with growing populations and rapid technological development in large countries such as China. The main point is that without replacing these energy sources before they run out, the world could face an energy catastrophe. Of all the energy sources available, the sun is the most abundant. One hour of sunlight

provides more energy than mankind consumes in a year. Yet even with such a huge potential, solar energy contributes less than 0.1% to the world's energy production. The major reason for such a low contribution is the high cost of solar photovoltaics compared to fossil fuels and even other renewable energy sources.

Due to the shortcomings of c-Si technology for PV applications including increasing prices and decreasing supply partially attributable to competition for the material with the computer industry, an alternative semiconductor absorber is desirable. The quaternary alloy copper indium gallium diselenide ( $\text{Cu(InGa)Se}_2$ ) (CIGS) and related materials in this copper chalcopyrite material class are very well developed for use in PV applications and offer vastly decreased thickness (decreasing weight and material), mechanical flexibility, superior and variable optoelectronics, higher efficiency, and lower deposition temperatures; all contributing towards potentially lowered energy costs. Because of its highly developed back ground as a PV material, there is already a wealth of knowledge regarding this material class that can be utilized to repurpose it for solar

*\*Corresponding author: M.Thirumoorthy, Department of Physics,  
Bannari Amman Institute of Technology, Sathy 638401, India*

cell applications. However, CIGS contains the elements Cu, In, Ga and Se. Amongst them, Gallium is a very scarcely available resource. Hence, alternative element Al can be used to form CuInAlSe<sub>2</sub>, this material can be a suitable alternative for CIGS Cu(In,Al)Se<sub>2</sub> thin films have been prepared by several techniques including co-evaporation (Marsillac et al., 2002; Reddy et al., 2006) one step RF magnetron sputtering (Badrul Munir et al., 2007), chemical bath deposition (CBD) (Kavitha and Dhanam,2007) and sequential deposition methods (Itoh et al., 1998). The co-evaporation technique gives the highest efficiency of Cu(In,Al)Se<sub>2</sub> based solar cells with 16.9% (Marsillac et al., 2001) but presents difficulties in upscaling. In this work, the pulse electrodeposition technique was employed for the first time to deposit CIAS thin films and the results are presented.

## 2.EXPERIMENTAL METHODS

In comparison to direct current electrodeposition, pulsed current (PC) electrodeposition is known to offer several benefits since it provides additional variables such as duty cycle and amplitude of pulsed current/potential. The duty cycle is defined as follows:

$$\text{Duty Cycle (\%)} = (\text{ON time}) / (\text{ON time} + \text{OFF time}) \times 100 \quad (1)$$

Appropriate regulation of these variables can be used for suitable manipulation of diffusion layer, grain size and nucleation. This, in twist, results in better deposit homogeneity as well as exact control over stoichiometry and deposition rate. During the deposition of thin films of ternary/quaternary systems, such control over the composition of individual elements is particularly crucial to obtain single-phase by controlling the formation of secondary phases, thereby making PC electrodeposition an attractive technique (Liu et al., 2011; Mandati et al., 2013a; Mandati et al., 2013b). Furthermore, by varying the duty cycle, reduction in porosity can be achieved by avoiding entrapment of hydrogen during deposition and results in a highly dense and compact films (Mandati et al., 2013b ;Mandati et al., 2014). In general, electrodeposition of Al and In is relatively difficult due to their more negative reduction potentials compared to Cu and Se. It has also been observed earlier, for copper indium gallium selenide (CIGS), that the In content decreases with increase in pulse off-time (low duty cycles), during the PC electrodeposition of CIGS thin-films (Liu et al., 2011; Mandati et al., 2013a). Due to these reasons, high concentration of Al and In precursor have been used to adjust the In and Al content in the films, in order to obtain stoichiometric CIAS thin films

CIAS thin films were deposited by the pulse plating technique using non aqueous ethylene glycol solution. 0.2 M Al<sub>2</sub>(SO<sub>4</sub>)<sub>3</sub>, 0.1 M In<sub>2</sub>(SO<sub>4</sub>)<sub>3</sub>, 0.02 M CuSO<sub>4</sub>, 0.05 M SeO<sub>2</sub>. The films were deposited at 80°C and at different duty cycles at a constant current density of 5 mA cm<sup>-2</sup>. Tin oxide coated glass (5 ohms/sq) were used as substrates. Conventional aqueous solutions cannot be always used as electrolytes due to the liberation of hydrogen molecule during electrolysis, narrow electrochemical windows, low thermal stability, and evaporation. These are the reasons why scientists have searched for non-aqueous solutions to electrodeposit thin films. Thickness of the films measured using Mitutoyo surface profilometer was in the range of 600 nm – 1100 nm

with increase of duty cycle from 6 – 50 %. The films were characterized by Xpertanalytical x-ray diffraction unit with CuK<sub>α</sub> radiation. Composition of the films was estimated by EDS attachment to JOEL SEM. Optical measurements were made at room temperature with Hitachi U3400 UV-VIS-NIR spectrophotometer. Photoelectrochemical cell measurements were made with 1 M polysulphide (1 M S, 1 M Na<sub>2</sub>S, 1 M NaOH) as the redox electrolyte with 250 W tungsten halogen lamp as the light source.

## 3.RESULTS AND DISCUSSION

The X-ray diffraction pattern of CIAS films formed at different duty cycles is shown in Fig.1. The films were polycrystalline exhibiting the peaks corresponding to the single phase CIAS.

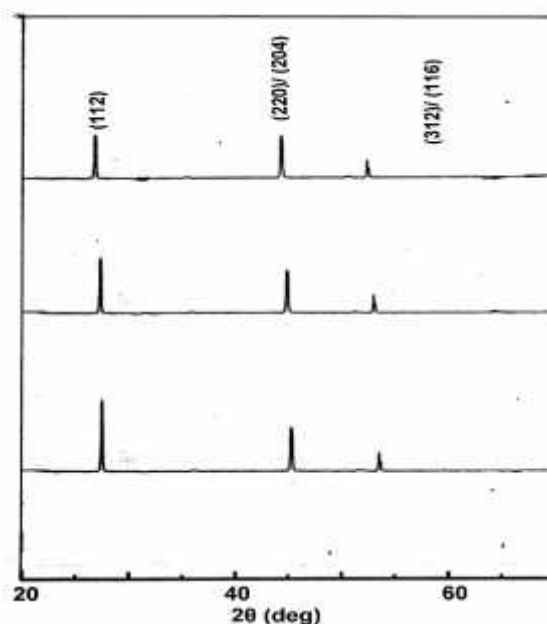


Fig.1 – X-ray diffraction pattern of CuIn<sub>0.7</sub>Al<sub>0.3</sub>Se<sub>2</sub> films deposited at different duty cycle Top – 9 % Middle – 33 % Bottom – 50 %

Peaks corresponding to (112), (220), (204), (312) and (116) orientations of the chalcopyrite structure were observed, similar to earlier reports (Bharath Kumar Reddy and Sundara Raja, 2006). The evaluated lattice parameters were around  $a = 5.644 \text{ \AA}$  and  $c = 11.135 \text{ \AA}$ . The crystallite size was calculated from the Full width half maximum of the diffraction profiles using Scherrer's equation

$$D = 0.95 \lambda / (\cos \theta) \quad (2)$$

Where, D is the crystallite size of the grains,  $\lambda$  is the wavelength of CuK<sub>α</sub> radiation ( $\lambda = 1.541 \text{ \AA}$ ),  $\Delta 2\theta$  is the full width at half maximum value,  $\theta$  is the Bragg angle, angle at which the diffraction occurs. The crystallite size increased from 17 nm – 42 nm as the duty cycle decreased from 50 % - 6 %. The crystallite size and thickness of the films are shown in Table.1.

The dislocation density  $\rho$ , defined as the length of dislocation lines per unit volume of the crystal has been evaluated using the formula (Santhosh Kumar and Pradeep, 2004)

$$\rho = 1/D^2 \quad (3)$$

The dislocation density is also presented in Table-1. From the table, it is identified that the dislocation density decreases with increase of crystalline grain size. Information on the particle size and strain for the CIAS films was obtained from the full-width at half-maximum of the diffraction peaks. The full-width at half-maximum can be expressed as a linear combination of the contributions from the particle size, D and strain, through the relation

$$\cos \theta / \sin \theta = 1/D + \sin \theta / \lambda \quad (4)$$

**Table.1 Structural parameters of CuIn<sub>0.7</sub>Al<sub>0.3</sub>Se<sub>2</sub> films deposited at different duty cycles.**

Duty cycle (%) (nm)	Thickness (nm)	Crystallite size (nm)	Internal stress (GPa)	Dislocation density (10 <sup>15</sup> linesm <sup>-1</sup> )
6	640	42	-0.25	0.56
9	750	34	-0.17	0.86
15	880	28	-0.15	1.27
33	1010	24	-0.07	1.73
50	1100	17	-0.02	3.46

The plot of  $\cos \theta / \sin \theta$  vs  $\sin \theta / \lambda$  allows us to determine both strain and particles size from slope and intercept of the graph. The calculated values of strain for CuIn<sub>0.7</sub>Al<sub>0.3</sub>Se<sub>2</sub> films deposited at different duty cycles ranges from 6 to 50% are listed in Table - 1.

The difference in the lattice parameter values from the bulk value experimental in the current case evidently suggest that the grains in the films are in stress. Such behaviour can be accredited to the change of nature, deposition conditions and the concentration of the native imperfections developed in thin films. This results in either elongation or compression of the lattice and the structural parameters. The density of the film is therefore found to change considerably in accordance with the variations observed with the lattice constant values. The defects have a probability to migrate parallel to the substrate surface so that the films will tend to expand and develop an internal tensile stress. This type of alteration in internal stress is always predominant by the identified in recrystallization process in polycrystalline films. The stress relaxation is mainly considered as due to dislocation glides formed in the films. The decrease of internal stress may be attributed to a decrease in dislocation density. The decrease in the strain and dislocation density with increase of duty cycle may be due to the decrease in concentration of lattice imperfections at superior duty cycle.

Composition of the films was determined by the Energy dispersive x-ray analysis (EDAX) attachment of the Scanning Electron Microscope (SEM). Decreasing the duty cycle from 50% to 15% reduces the relative content of Al and Se, but has no obvious effect on Indium relative content in the film, this can be attributed to the fact that Al was first dissolved back into the solution due to its lowest electronegativity corresponding to the positive current during the nonpulse duration  $t_{off}$ , leading to the loss of Al in the deposited film, and therefore reduction of Al-Se compound(s). Similar phenomenon also has been observed during the pulse electrodeposition of ternary CuInSe<sub>2</sub> (Endo et al., 1996).

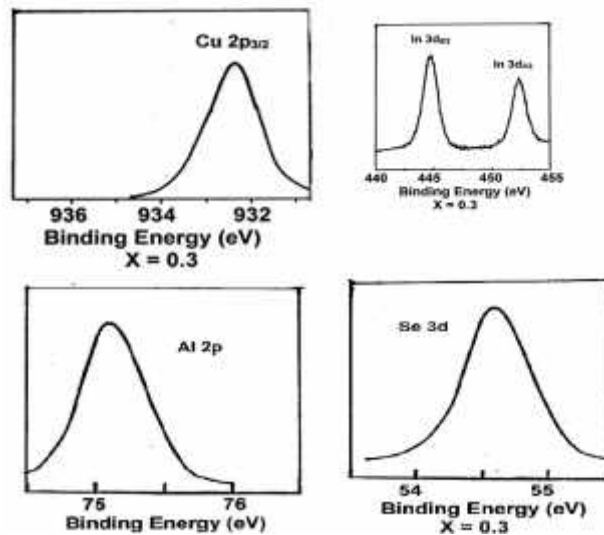


**Fig. 2 EDAX spectrum of CuIn<sub>0.7</sub>Al<sub>0.3</sub>Se<sub>2</sub> films of different composition deposited at 50 % duty cycle**

When duty cycle further decreases to 6 %, besides significant loss of Al, the relative content of indium also indicates some drop, thereby leading to a corresponding reduction of In-Se compound(s). Due to the above-mentioned reasons, the composition of the films deposited at 50 % duty cycle was CuIn<sub>0.7</sub>Al<sub>0.3</sub>Se<sub>2</sub>, which decreased to CuIn<sub>0.72</sub>Al<sub>0.28</sub>Se<sub>2</sub> at 33 % duty cycle, and to CuIn<sub>0.78</sub>Al<sub>0.22</sub>Se<sub>2</sub>, CuIn<sub>0.76</sub>Al<sub>0.24</sub>Se<sub>2</sub>, CuIn<sub>0.77</sub>Al<sub>0.23</sub>Se<sub>2</sub> for 15 %, 9 % and 6 % duty cycle respectively.

XPS spectra of as-deposited CuIn<sub>0.7</sub>Al<sub>0.3</sub>Se<sub>2</sub> films are shown in Fig. 3. The binding energy (B.E.) values of Cu 2p<sub>3/2</sub>, In-3d<sub>5/2</sub> and 3d<sub>3/2</sub>, Al 2p and Se-3d peaks in the XPS spectra were observed.

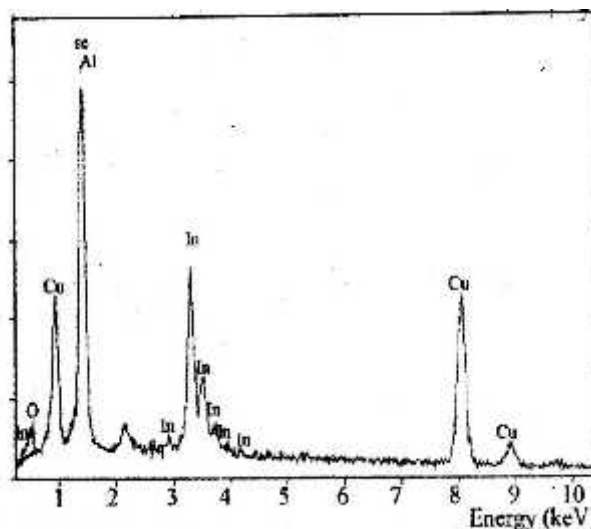


**Fig. 3 XPS spectra of CuIn<sub>0.7</sub>Al<sub>0.3</sub>Se<sub>2</sub> films deposited at 50 % duty cycle**

The B.E. value of Al 2p 75.1 eV with for the value X = 0.3. Similarly, the Indium B.E. values of In (3d<sub>3/2</sub>) and In (3d<sub>5/2</sub>) 452.5 eV and from 445 eV respectively as the x value is equal to 0.3. The BE value of Se – 3d is 54.6 eV ‘x’ value equals to 0.3. The Cu 2p<sub>3/2</sub> BE value of 932.2 eV obtained for the x-value is equal to 0.3. The above values are like those obtained for CuInAlSe<sub>2</sub> films deposited by one step electrodeposition (Deepa et al., 2014).

Surface morphology of the CuIn<sub>0.7</sub>Al<sub>0.3</sub>Se<sub>2</sub> films of deposited at 50% duty cycle is studied by Atomic force microscopy. Fig. 4 shows the atomic force micrographs of the films of deposited at 50% duty cycle. It is observed, that as the aluminium concentration increases, the grain size decrease and the surface becomes smooth. The rms value of surface roughness value obtained as 0.6 nm as the aluminium concentration increases. The increase of surface roughness is due to increase of grain size.

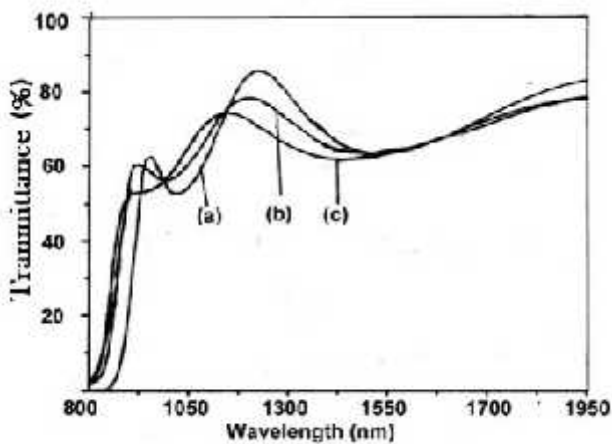


Fig. 4 Atomic force micrograph of CuIn<sub>0.7</sub>Al<sub>0.3</sub>Se<sub>2</sub> films deposited at 50% duty cycle X – 200 nm x 200 nm, Z – 1 div – 1 nm

Fig. 5 shows the transmittance spectra of the CuIn<sub>1-x</sub>Al<sub>x</sub>Se<sub>2</sub> films of deposited at 50 % **RMS = 0.6 nm**

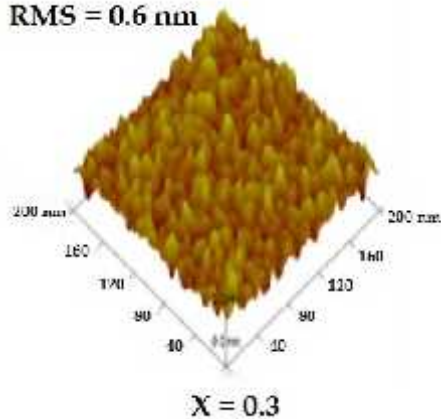


Fig. 5 Transmittance spectra of CuIn<sub>1-x</sub>Al<sub>x</sub>Se<sub>2</sub> films of different composition (a) x = 0.3 (b) x = 0.2 (c) x = 0.1

The spectrum exhibits interference fringes and the value of the refractive index was estimated by the envelope method (Swanepoel, 1983).

$$n = [N + (N^2 - n_s^2)]^2 \quad (5)$$

$$N = (n_s^2 + 1)/2 + 2 n_s (T_{max} - T_{min}) / T_{max} T_{min} \quad (6)$$

where n<sub>s</sub> is the refractive index of the substrate, T<sub>max</sub> and T<sub>min</sub> are the maximum and minimum transmittances at the same wavelength in the fitted envelope curve on a transmittance spectrum. The value of the refractive index, calculated from the equations 3 and 4 was in the range of 2.75 - 2.77 for the samples of deposited at different composition X = 0.1, 0.2 and 0.3 at 50% duty cycle.

The value of the absorption co-efficient (α) was calculated using the relation

$$\alpha = 1/d \ln \{ (n-1)(n-n_s)/(n+1)(n-n_s) \} [ (T_{max}/T_{min})^2 + 1 ] / [ (T_{max}/T_{min})^2 - 1 ] \quad (7)$$

where ‘d’ is the thickness of the CIAS film and the other parameters have the common meaning as given for equation (4). The films exhibited a high absorption co-efficient of the order of 10<sup>4</sup> cm<sup>-1</sup>.

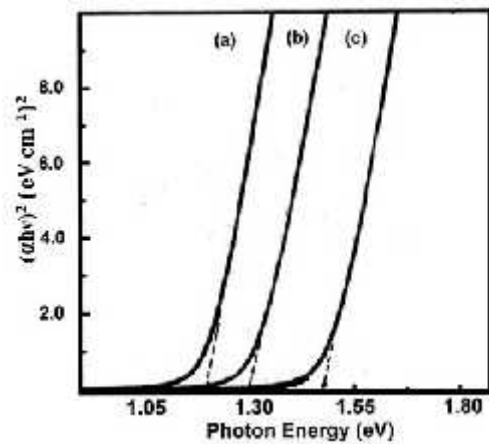


Fig. 6 Tauc's plot of CuIn<sub>1-x</sub>Al<sub>x</sub>Se<sub>2</sub> films of different composition (a) x = 0.1 (b) x = 0.2 (c) x = 0.3 at 50% duty cycle.

A plot of (αhν)<sup>2</sup> against hν, as indicated in Fig.6, exhibits linear behavior near the band edge, the band gap of the deposited films was determined to be in the range of 1.17 – 1.51 eV. This value agrees well with earlier report on thermally evaporated CuIn<sub>0.7</sub>Al<sub>0.3</sub>Se<sub>2</sub> films (Smaili et al., 2008).

Photoelectrochemical (PEC) cells were prepared using the films deposited at 80°C and at different duty cycles. The CIAS films were lacquered with polystyrene to prevent the metal substrate portions from being exposed to the redox electrolyte. These films were used as the working electrode. Photoelectrochemical cell studies were made using 1.0 M Na<sub>2</sub>S, 1.0 M NaOH and 1.0 M S, as the redox electrolyte. Graphite was used as the counter electrode. The ORIEL 250 W tungsten Halogen lamp is used as the light source used for illumination.

A water filter was introduced between the PEC cell and the light source to cut off the InfraRed portion. By using CEL suryamapi, the intensity of illumination of light was measured, whose readings are directly regulated in mWcm<sup>-2</sup>.



The intensity of illumination was varied changing the distance between the source and the cell. The PEC cells power output characteristics was measured by connecting the ammeter and resistance box in series and the output voltage was measured across the load resistance. The dark current, output voltage and photocurrent were measured with a HIL digital multimeter.

The CIAS photoelectrodes were dipped in the electrolyte and allowed to attain equilibrium under dark conditions for about 10 minutes. The dark current and voltage values were noted. The cells were then illuminated by the light source and the current and voltage were measured for each setting of the resistance box. The photocurrent and photovoltage were calculated as the difference between the current under illumination and the dark current, and voltage under illumination and dark voltage respectively. The intensity of the light falling on the films deposited at different duty cycles was kept constant at  $60 \text{ mW cm}^{-2}$ .

Illumination of the interface with light of suitable wavelength that shows a photovoltaic effect is an important technique to determine the properties of semiconductor/electrolyte interfaces. The PEC cells using these films exhibited very low photocurrent and photovoltage. Amongst the films deposited at different duty cycle, films deposited at 50 % duty cycle exhibited maximum photocurrent and photovoltage. Hence, further studies were made on the films deposited at 50 % duty cycle. The  $\text{CuIn}_{0.7}\text{Al}_{0.3}\text{Se}_2$  films shown low photoactivity, amongst the films, those deposited at 50 % duty cycles shown maximum photo output. The films deposited at 50 % duty cycle photo output parameter increase, as the film post heated in argon atmosphere at various temperatures in the range of  $450 - 525^\circ\text{C}$  for 15 min.

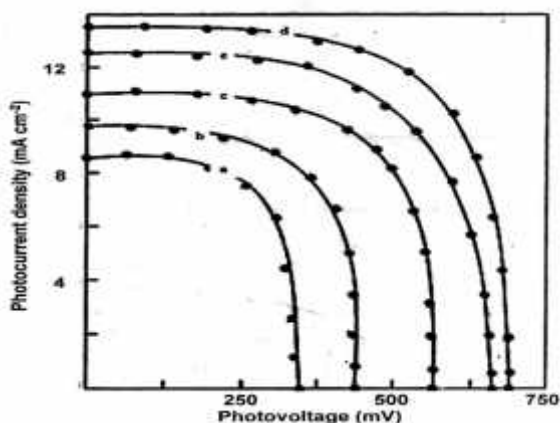


Fig.7 – Load characteristics of CIAS films deposited at 50 % duty cycle and post heated at different temperatures (a)  $450^\circ\text{C}$  (b)  $475^\circ\text{C}$  (c)  $500^\circ\text{C}$  (d)  $525^\circ\text{C}$  (e)  $550^\circ\text{C}$

Fig.7 shows the load characteristics of the post heat treated films. From the figure, PEC output parameters, viz., short circuit current and open circuit voltage were found to increase for the temperature heat-treated upto a  $550^\circ\text{C}$ . Lower open circuit voltage and short circuit current will be obtained when the Photoelectrodes heat-treated at temperatures greater than  $525^\circ\text{C}$  is mainly due to the slight change in stoichiometry and

reduction in thickness of the films. The photovoltaic parameters are shown in Table II.

Table – II Photovoltaic parameters of  $\text{CuIn}_{0.7}\text{Al}_{0.3}\text{Se}_2$  films deposited at 50 % duty cycle and post heat treated at different temperatures (Intensity –  $60 \text{ mW cm}^{-2}$ )

Heat treatment Temp ( $^\circ\text{C}$ )	$V_{oc}$ (mV)	$J_{sc}$ ( $\text{mA cm}^{-2}$ )	ff (%)	$R_s$ ( $\Omega$ )	$R_{sh}$ (k $\Omega$ )
450	360	8.40	0.55	3.56	40
475	450	9.80	0.58	4.02	37
500	570	11.00	0.63	5.42	31
525	670	13.50	0.68	7.69	9
550	630	12.30	0.64	8.75	14
525	750	21.00	0.62	12.21	5

(After photoetch)

For a film deposited at 50 % duty cycle and post heat treated at  $525^\circ\text{C}$ , a short circuit current density of  $13.5 \text{ mA cm}^{-2}$  and open circuit voltage of  $0.67 \text{ V}$  were observed at  $60 \text{ mW cm}^{-2}$  illumination. Both  $V_{oc}$  and  $J_{sc}$  increased with increase of intensity. Beyond  $80 \text{ mW cm}^{-2}$  illumination,  $J_{sc}$  is found to linearly increase with intensity of illumination and  $V_{oc}$  was found to saturate as normally observed in the PEC cells and photovoltaic cells. A plot of  $\ln J_{sc}$  vs  $V_{oc}$  yielded a straight line. Extrapolation of the line to the y-axis yields a  $J_0$  value of  $1.8 \times 10^{-7} \text{ A cm}^{-2}$ , the ideality factor (n) was calculated from the slope of the straight line and it was found to be 1.75.

Photoetching was done by shorting the photoelectrodes and the graphite counter electrode under an illumination of  $100 \text{ mW cm}^{-2}$  in  $1 : 100 \text{ HNO}_3$  for different durations in the range  $0 - 100\text{s}$ . Both photocurrent and photovoltage are found to increase up to  $80\text{s}$  photoetch, beyond which they begin to decrease. This is illustrated in Fig.8 for the photoelectrode deposited at 50 % duty cycle. The decrease of the photocurrent and

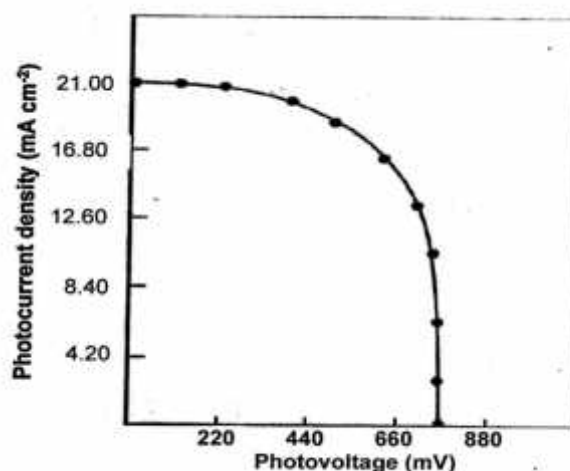


Fig.8 – Load characteristics of  $\text{CuIn}_{0.7}\text{Al}_{0.3}\text{Se}_2$  films deposited at 50% duty cycle and post heat treated at  $525^\circ\text{C}$  after photoetching for 80 s

photovoltage after 80s photoetch may be attributed to separation of grain boundaries due to prolonged photoetching (Mangalhari et al.1988).

The power output characteristics (Fig.8) indicates a  $J_{sc}$  of  $21.00 \text{ mA cm}^{-2}$ ,  $V_{oc}$  of  $0.75\text{V}$ , ff of  $0.62$  and  $\eta$  of  $12.21\%$ , for  $60 \text{ mW cm}^{-2}$  illumination after 80s photoetching. The photovoltaic parameters of the electrodes with and without photoetching are shown in Table.2.

Photoetching process successfully decreases the density of recombination centers by etching out surface steps and imperfections. This leads to improvement in photocurrent by greater than three times and hence conversion efficiencies will improved. It was found that surface steps, inhomogenities and defects are etched/removed because of photoetching. The photoetching process has been generally found to result in a slight increase in the photovoltage (open circuit voltage). This has been found to be a consequence of the change in flat band potential.

Photoetching is apparently one of the most promising surface treatment process for enhancement of conversion efficiency through suppression of recombinations. The fill factor (FF) is another important PEC parameter which manifests the solar-to electrical energy conversion efficiency of the cell. It reflects the ability of photogenerated current to perform work through an external load and is therefore very sensitive to the kinetics of current flow through the semiconductor/electrolyte interface. It has been found that in addition to photocurrent, the fill factor gets enhanced, but to a lesser degree as a result of photoetching. The dominant reason for this is thought to be a decrease in recombination velocity of minority carriers. The improvement in the fill factor indicates the fact that the semiconductor/electrolyte interface behaves closer to the ideal case after photoetching, i.e., the dark saturation current decreases (shunt resistance increases), (series resistance decreases). Because of photoetching reflectivity decreases and absorptivity of light increases it leads to a better conversion efficiency. It is thought that the decrease in reflectivity occurs due to the formation of microetch pits on the electrodes and hence a roughening of the surface steps upon photoetching. Similar behaviour was observed in  $\text{WSe}_2$  photoelectrodes (Prasad and Srivastava, 1988).

#### 4.CONCLUSIONS

Single phase nanocrystalline  $\text{CuIn}_{0.7}\text{Al}_{0.3}\text{Se}_2$  films could be deposited by the pulse electrodeposition technique. The band gap of the films can be adjusted from  $1.17 \text{ eV}$  to  $1.51 \text{ eV}$  with increase of duty cycle. Photoelectrochemical solar cells exhibiting  $12.21 \%$  efficiency can be fabricated with the films.

#### 5.REFERENCES

Badrul Munir, Rachmat A Wibowo, Eun Soo Lee and Kyoo Ho Kim.2007. 'One step deposition of  $\text{Cu}(\text{In}_{1-x}\text{Al}_x)\text{Se}_2$  thin films by RF magnetron sputtering', Journal of Ceramic Processing Research, **8**(4), 252-255.

Bharath Kumar Reddy, Y and Sundara Raja, V. 2006, 'Preparation and Characterization of  $\text{CuIn}_{0.3}\text{Al}_{0.7}\text{Se}_2$  Thin

Films for Tandem Solar Cells', Solar Energy Materials and Solar Cells, vol. 90, no. 11, pp. 1656-1665.

Deepa, K.G., Lakshmi Shruthi, N., Anantha Sunil, M. and Nagaraju, J. 2014. 'Cu(In,Al)Se<sub>2</sub> thin films by one-step electrodeposition for photovoltaics', Thin Solid Films, vol.551, pp. 1-7.

Endo, S., Nagahori, Y. and Nomura, S. 1996,'Preparation of  $\text{CuInSe}_2$  films by pulse electrodeposition', Japanese Journal of Applied Physics vol.85, no.9A, pp.L1101 – L1103.

Itoh, F., Saitoh, O., Kita, M., Nagamori, H. and Oike, H.1998. 'Growth and Characterization of  $\text{Cu}(\text{In,Al})\text{Se}_2$  by vacuum evaporation', Solar Energy Materials and Solar Cells, **50**(1-4), 119-125.

Karaagac, H., Kaleli, M. and Parlak, M. 2009. 'Characterization of  $\text{AgGa}_{0.5}\text{In}_{0.5}\text{Se}_2$  thin films deposited by electron-beam technique', Journal of Physics D: Applied Physics, vol.42, no.16, pp.5413.

Kavitha, B. and Dhanam. M. 2007. 'In and Al composition in nano  $\text{Cu}(\text{InAl})\text{Se}_2$  thin films from XRD and transmittance spectra', Materials Science And Engineering: B, **140**(1), 59-63.

Liu, F., Huang, C., Lai, Y., Zhang, Z., Li, J. and Liu, Y. 2011, 'Preparation of  $\text{CuInGaSe}_2$  films by pulse electrodeposition', Journal of Alloys Compound, vol.509, no.8, pp. L129-L133.

Mandati, S., Sarada, B.V., Dey, S.R. and Joshi, S.V. 2013a. 'Pulse electrodeposition of  $\text{CuInSe}_2$  films with morphology for solar cells', Journal of Electrochemical Society, vol.160, no.4, pp. D173-D177.

Mandati, S., Sarada, B.V., Dey, S.R. and Joshi, S.V. 2013b. 'Improved photoelectrochemical performance of  $\text{CuInGaSe}_2$  thin films prepared by pulse electrodeposition', Journal Renewable & Sustainable Energy Reviews vol.5, no.3, pp.031602.

Mandati, S., Sarada, B.V., Dey, S.R., Joshi, S.V. 2014,' $\text{CuInGaSe}_2$  films for photovoltaic solar cell applications by two stage pulse current electrodeposition', Materials Letters, vol.118, pp.158 – 160.

Mangalhari, J.P., Thangaraj, R. and Agnihotri, O.P. 1988. 'Photoelectrochemical Conversion Using Sprayed  $\text{CdSe}$ ', Bulletin of Material Science, vol.10, no.4, pp. 333-340.

Marsillac, S., Paulson, P. D., Haimbodi, M. W., Birkmire, R. W. and Shafarman, W. N. 2002.High-efficiency solar cells based on  $\text{Cu}(\text{InAl})\text{Se}_2$  thin films', Applied Physics Letters **81**(7), 1350.

Marsillac, S., Wahiba, T. B., Moctar, C., Bernède, J. C. and Khellil, A.2001. 'Evolution of the properties of  $\text{CuAlSe}_2$  thin films with the oxygen content', Solar Energy Materials and Solar Cells, vol.71, pp. 425-434.

Prasad, G. and Srivastava, O.N. 1988. 'The high-efficiency (17.1%)  $\text{WSe}_2$  photo-electrochemical solar cell', Journal of Physics D: Applied Physics, vol.21, no.6, pp. 1028.

Reddy, Y. B. K., Raja, V. S. and Sreedhar, B.2006. 'Growth and characterization of  $\text{CuIn}_{1-x}\text{Al}_x\text{Se}_2$  thin films deposited by coevaporation', Journal of Physics D: Applied Physics **39**(24), 5124.

Santhosh Kumar, M.C. and Pradeep, B. 2004, 'Formation and properties of  $\text{AgInSe}_2$  thin films by co-evaporation', Vacuum, vol.72, no.4, pp.369-378.

Smaili, F., Kanzari, M. and Rezig, B. 2008. 'Characterization of  $\text{CuInAlSe}_2$  films prepared by thermal evaporation', Materials Science and Engineering C vol.28, no.5-6, pp. 954-958.

Swanepoel, R. 1983. 'Determination of the thickness and optical constants of amorphous silicon', Journal of Physics E: Scientific Instruments, vol.16, pp. 1214-1222.